Method of achieving a wide field-of-view head-mounted display with small distortion

Jianming Yang,[1,2] Weiqi Liu,[2,*] Weizhen Lv,[1,2] Daliang Zhang,[2] Fei He,[2] Zhonglun Wei,[2] and Yusi Kang[2]

[1]*University of Chinese Academy of Sciences, Beijing 100049, China*

[2]*Changchun Institute of Optics, Fine Mechanics and Physics, Chinese Academy of Sciences, Changchun, Jilin 130033, China*

**Corresponding author: liuwq@ciomp.ac.cn*

Received May 8, 2013; accepted May 10, 2013;
posted May 13, 2013 (Doc. ID 190266); published June 4, 2013

We present a method of achieving a wide-angle, lightweight, optical see-through, distortion-free head-mounted display (HMD) by using two similar ellipsoids. An HMD that achieves a single channel field-of-view (FOV) of $120° \times 120°$ with a 6 mm eye box and a total binocular FOV of $160° \times 120°$ with an 80° field overlap is designed as an example. This method can solve the complex tiling problem and the distortion problem of other catadioptric structures. This structure is used to offset distortion and correct aberrations.

OCIS codes: (080.2740) Geometric optical design; (220.3620) Lens system design; (330.7322) Visual optics, accommodation.

http://dx.doi.org/10.1364/OL.38.002035

Developing a wide field-of-view (FOV) head-mounted display (HMD) has been a great technological challenge for decades. An early attempt at extending the FOV was the LEEP Optical System [1]. The challenge has been to provide high-quality panoramic imagery in a lightweight and compact package. Tiling is another approach to achieve a wide FOV and high resolution with minimum image distortion. For example, the full-immersion HMD by Arthur [2] achieved a binocular FOV (BFOV) of $176° \times 47°$ by using 3×2 display units per eye. However, the center of the field curvature of this model was at the apex of the cornea rather than at the eye rotation center, thereby breaking the seamless image with eye movements. This problem has been solved by the Sensics piSight display by using the patent technology developed by Massof *et al.* ($\mathrm{BFOV} = 179° \times 58°$) [3]. The free-form surface prism HMD by Yamaska has been widely used [4]. Cheng *et al.* achieved a BFOV of $119° \times 56°$ with an 8 mm eye box by using a 3×2 free-form prism [5]. The advantage of tiling is that it can easily achieve a large FOV with high resolution, a large eye box, and a small distortion. The major difficulty for optical tiling is positioning the image generator windows to provide good alignment and a smooth image across the tiles.

A catadioptric system, which can reduce system size and weight in HMDs, is another important research direction. Sisodia and co-workers achieved a high-BFOV ($100° \times 50°$) rotationally symmetric system with a 50 mm eye relief and a 15 mm eye box size on the basis of nodal aberration theory [6,7]. Other catadioptric systems are summarized in [8]. All of these systems use one combiner and several lenses. Given that the distortion produced by the combiner in this system is significant, good image quality is difficult to achieve if strict requirements are imposed on the distortion. The distortion problem has been solved not optically but electronically by remapping the image with a renderer [9].

Motivated by the above mentioned studies, we propose a wide FOV, lightweight, large eye relief HMD (see Fig. 1). Table 1 lists the performance parameters of the proposed HMD.

The optics includes two ellipsoidal concave mirrors, a relay lens, and an imaging lens. Figure 1 shows the components and optics of the proposed HMD. The two ellipsoids have the same conic coefficient but different radii. We can find a similar structure in [10]. The distance between the right focus of the left ellipsoid and the left focus of the right ellipsoid is restricted within a small range. Therefore, the system maintains symmetry, which can offset the distortion generated by the right ellipsoid. The relay lens is located between the two ellipsoids and the imaging lens at the left focus of the left ellipsoid.

Figure 2(a) shows the top view of the system after the unnecessary parts of the ellipsoids are removed. The system is optimized with rays traced from the eye position to the microdisplay in ZEMAX. The virtual image of the HMD can be designed to infinity or several meters in front of the viewer to ensure that parallel or nearly parallel rays enter the eyes. Figure 2(b) shows the result when parallel rays at 120° enter into the schematic eye proposed by Sanz and Navarro [11]. For an FOV of 120°, peripheral rays generate an immersive feeling with poor image quality when the eye gazes at the center field. Eye rotation is required if the viewer is interested in the marginal fields. The total length of the system is 150 mm. A 3 mm thick aluminum is used as material of the reflecting surfaces. The total weight of the system

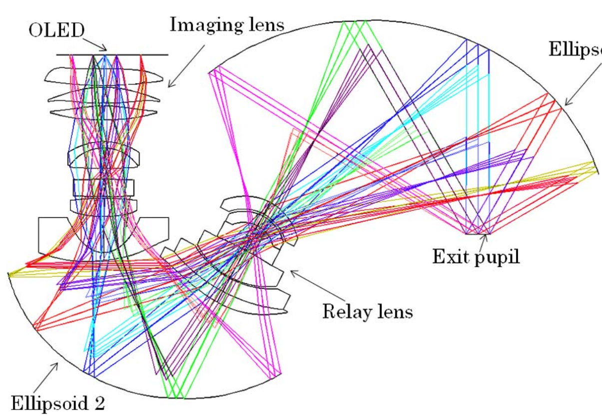

Fig. 1. System components and optics.

Table 1. Performance Parameters

Parameter	HMD
Field-of-view ($H \times V$)	$120° \times 120°$ (monocular) $160° \times 120°$ (80° overlap)
Eye clearance distance (mm)	16
Eye relief (mm)	49 (on the pupil axis)
Eye box (mm)	6
Resolution (arcmin)	3.75
Maximum distortion (%)	2.2
MTF system	$\geqq 0.1$ *at* 50 lp/mm
Length (mm)	150
Weight (g)	226

is 226 g, and the mass center is located at MC in Fig. 2(d). Figures 2(c) and 2(d) show the effect of wearing an HMD with real ratio to the human head.

Figure 3(b) presents the minimum distortion when an angle exists between an image and object planes (known as the Scheimpflug condition) [12]. Such distortion is difficult to correct by simply placing refractive lenses around the second focus. To solve this problem, another ellipsoid with the same conic constant is used to offset the distortion caused by the first ellipsoid [see Fig. 3(c)]. The right focus of the left ellipsoid overlaps with the left focus of the right ellipsoid. Lights emitted from focus A converge to focus B. Rays then converge to focus C because focus B is also a focus of the left ellipsoid. The two ellipsoids have the same conic constant. Thus, $\Delta ADB \approx \Delta CEB$, $CE \| DA$. In addition, an arbitrary angle α at focus A is equal to the corresponding angle β at focus C (i.e., $\alpha = \beta$). Therefore, the image at FG forms a distortionless image at HL if no other lens exists. The grid distortion is shown in Fig. 3(d).

The property of the ellipsoid is narrowly appropriate for pointolite at one focus. However, only the chief ray can converge to the second focus when parallel light with a cross section (a circle 6 mm in diameter) is emitted from the first focus. The diameter D of each field in the section reaches a maximum L on the second

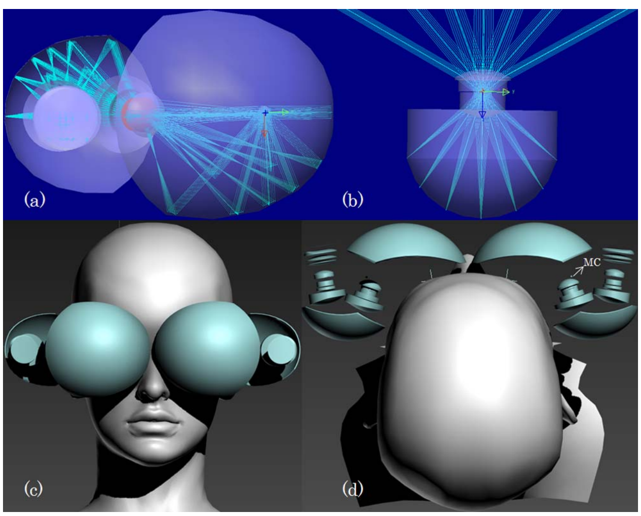

Fig. 2. (a) Top view of the system. (b) Effect of schematic eye in large FOV. (c) Front view of wearing. (d) Lateral view of wearing with mass center.

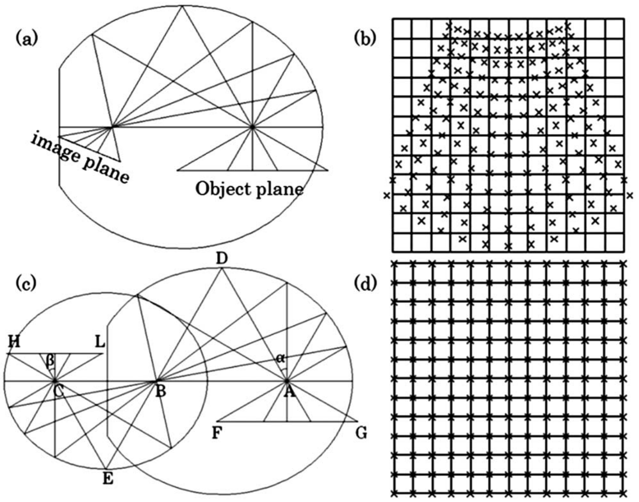

Fig. 3. (a) Chief rays of just one ellipsoid. (b) Minimum distortion when an angle exists between an image plane and an object plane. (c) Structure of two ellipsoids. (d) Free grid distortion.

ellipsoid, as shown in Fig. 4(a). The tangential curvature of the ellipsoid varies from the sagittal curvature along the long axis. Therefore the larger the ray section is on the second ellipsoid, the greater the astigmatism, the coma, and the full beam divergence θ are generated.

The large astigmatism, coma, and divergence θ result in difficulty in producing good image quality. Thus, a relay lens that can concentrate light to reduce the ray section on the second ellipsoid and can cause minimal change to the chief ray of each field is set between the two ellipsoids. Figure 1 shows this effect. The distortion caused by the relay lens does not matter because the lens is designed to have a correctable change in the chief ray and to have positive focal power. Figure 4(b) shows a ball-like lens around the common focus, which is considered the simplest structure with no effect on the chief ray. However, this lens causes large curvature. The green field focuses on M, whereas the red field diverges. A single lens also causes color aberration. Thus, the relay lens is designed to contain several lenses with different glasses to correct field curvature and color aberrations.

To enhance the handling of chief rays, the imaging lens starts under the left focus of the left ellipsoid before the chief rays converge to the focus, thus reducing the difficulty in correcting distortion. The maximum distortion of the system within 120° is limited to 2.2%, a requirement that can be reduced according to actual demands. Three plane-symmetry xy-polynomial surfaces with a maximum

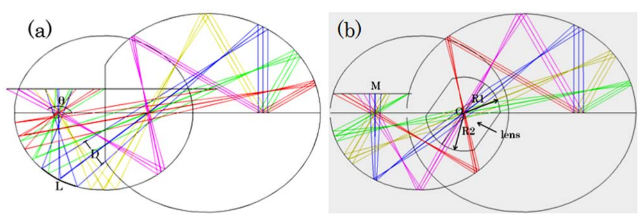

Fig. 4. (a) Beam path of parallel light with section reflected by two ellipsoids without relay lens. (b) Chief ray of every field with ball-like relay lens.

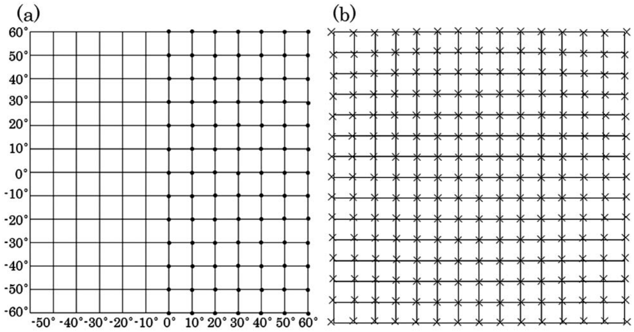

Fig. 5. (a) Points to be optimized and (b) grid distortion.

order of 8 are used because of the asymmetry of the ellipsoid along the long axis. In freeform systems, the performance in the design field points is usually excellent; however, the performance in fields between these points is usually poor. The optimization is taken on 7×13 grid points emphasized on the left side of Fig. 5(a) under the design wavelength (486.1, 587.6, and 656.2 nm) to guarantee excellent overall performance. All field angles are uniformly distributed within $60° \times 120°$ angle space and within $120° \times 120°$ because the system is single-plane symmetric. Figure 5(b) shows the grid distortion. The maximum distortion in the microdisplay path is 2.2%.

Figure 6 plots the modulation transfer functions (MTFs) of 24 fields within 91 grid points. The MTFs of all fields are above 0.1 at 50 lp/mm. To assess the quality of the final image, a 2D image simulation is conducted, as shown in Fig. 7(b). Compared with those in the original image, the distortion and chromatic aberration in the simulated picture are effectively corrected. The peripheral fields are weakly illuminated because the numerical aperture of the center fields on the microdisplay path is much larger. The luminous intensity of the microdisplay should be reconstructed to achieve uniform brightness.

HMDs generally seek a wide FOV and high resolution. However, given that the displays in an HMD are magnified to achieve a larger FOV, the pixels on the display are magnified, resulting in a trade-off between the FOV and resolution. Resolution can be increased by reducing pixel size and increasing image size. The proposed design is based on the highest-resolution active-matrix organic light-emitting diode microdisplay from eMagin. The image size is a square with a side length of 18.7 mm, which is different from the product because the product has a ratio of 16:9. The resolution of the HMD is 3.75 arcmin. If a larger microdisplay with a side length of 30 mm is produced, then the resolution will be 2.3 arcmin with the same pixel size of 9.6 μm. However, the design must be changed to fit the new microdisplay.

A method of achieving a wide FOV, lightweight, large eye relief, optical see-through HMD by using two similar

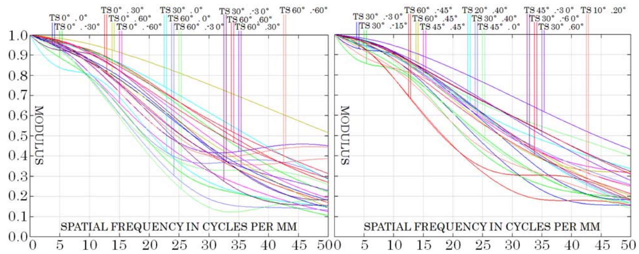

Fig. 6. (a) MTF plots of the eyepiece.

Fig. 7. (a) Original and (b) simulated pictures.

ellipsoids is proposed for the first time. The HMD is expected to be useful not only in virtual reality applications, such as simulation training, but also in entertainment because of the immersive feeling HMD provides. The method can be applied to design HMDs with different parameters, such as with reduced FOV and with enlarged eye box, to meet different requirements. Future works should aim to create a rotationally symmetric system.

References

1. E. M. Howlett, Proc. SPIE **1669**, 193 (1992).
2. K. W. Arthur, *Effects of Field of View on Performance with Head-Mounted Displays* (University of North Carolina at Chapel Hill, 2000).
3. L. G. Brown and Y. S. Boger, in *SID International Symposium Digest of Technical Papers* (Society for Information Display, 2008), Vol. **39**, p. 77.
4. S. Yamazaki, K. Inoguchi, Y. Saito, H. Morishima, and N. Taniguchi, Proc. SPIE **3639**, 453 (1999).
5. D. Cheng, Y. Wang, H. Hua, and J. Sasian, Opt. Lett. **36**, 2098 (2011).
6. A. Sisodia, M. Bayer, P. T. Smith, B. Nash, J. Little, W. Cassarly, and A. Gupta, Proc. SPIE **6557**, 65570N (2007).
7. A. Sisodia, A. Riser, and J. R. Rogers, Proc. SPIE **5801**, 304 (2005).
8. O. Cakmakci and J. P. Rolland, J. Disp. Technol. **2**, 199 (2006).
9. A. Bauer, S. Vo, K. Parkins, F. Rodriguez, O. Cakmakci, and J. P. Rolland, Opt. Express **20**, 14906 (2012).
10. D. Shafer, Adv. Opt. Technol. **2**, 53 (2013).
11. I. E. Sanz and R. Navarro, J. Opt. Soc. Am. **16**, 1881 (1999).
12. J. M. Sasian, Opt. Eng. **31**, 527 (1992).